Sensors and Materials, Vol. 32, No. 12 (2020) 4121–4129
MYU Tokyo

S & M 2398

Flexible Hybrid Electronic Device Sealed by Dimethylpolysiloxane with Floating Nested Structure

Toshihiro Takeshita,* Takahiro Yamashita, Yusuke Takei, and Takeshi Kobayashi

National Institute of Advanced Industrial Science and Technology (AIST),
1-2-1 Namiki, Tsukuba, Ibaraki 305-0028, Japan

(Received March 18, 2020; accepted April 24, 2020)

Keywords: FHE, MEMS, ultrathin chip, stretchable electronics, flexible electronics

This paper describes a new sealing structure, a "floating nested structure", for flexible hybrid electronic (FHE) device applications using an ultrathin chip (UTC). In the floating nested structure, the part on which the UTC is mounted is physically connected to the sealing material only with a meander structure. By using the floating nested structure, the tensile strain transmitted to the UTC mounted on a flexible substrate can be reduced markedly. We fabricated a UTC with a thickness of 5 μm using deep reactive ion etching (deep-RIE) technology. The fabricated UTC had flexibility with a radius of curvature of 0.5 mm. Also, we conducted an experiment to demonstrate the effect of the floating nested structure. When the elongation of the test sample used in the experiment was 20%, the strain on the flexible substrate without the floating nested structure was 710 με. In contrast, the strain was 220 με when using the flexible substrate with the floating nested structure. This means that the floating nested structure reduced the propagation of strain by 69.0%. From the above results, it is expected that the floating nested structure can be useful in the development of FHE devices with both elasticity and flexibility.

1. Introduction

Flexible electronic devices have been developed as key devices in the field of the Internet of Things (IoT). In particular, flexible electronic technologies are expected to be used in healthcare monitoring applications such as electrocardiogram,[1–3] pulse wave,[4,5] myocardium,[6,7] muscle sound,[8] blood flow meter,[9,10] and thermometer[11,12] monitoring. This is because flexible electronic technologies enable the fabrication of healthcare monitoring devices that are comfortable to wear. To realize both flexible and stretchable electronics, printed electronic devices using organic materials, molecular materials, and nanowire substrates were previously studied.[13] However, printed electronic devices have many problems with regard to functionality, reliability, and durability.

In contrast, conventional silicon-based electronic devices have the advantages of good functionality and high reliability. However, they are hard, brittle, and inflexible. Therefore, a technology called flexible hybrid electronics (FHE) has been receiving attention. This

*Corresponding author: e-mail: toshihiro-takeshita@aist.go.jp
https://doi.org/10.18494/SAM.2020.2874

ISSN 0914-4935

technology achieves both flexibility and good functionality by combining an ultrathin chip (UTC) consisting of single-crystal silicon and printed electronics. When a silicon-based electronic device is thinned to a thickness of less than 20 μm by chemical mechanical polishing (CMP), dry etching, and MEMS processing,[14–18] it becomes flexible. Vanfleteren's group fabricated an ultrathin microcontroller unit (MCU) with flexibility and good performance,[19,20] and demonstrated that an MCU with a thickness of 20 μm can operate when its radius of curvature is 3.3 mm. Additionally, it was demonstrated that the effect of bending can be reduced by thinning.

However, although a UTC is flexible, it does not have stretchability. Moreover, a UTC easily breaks when tensile stress is applied to it. To make the UTC stretchable, a meander structure is generally formed on a flexible substrate,[21,22] as shown in Fig. 1. This meander structure absorbs the tensile stress and reduces the transmission of tensile strain to the island structure on which the UTC is mounted. Additionally, we previously demonstrated that it is possible to reduce the strain transmission using a floating island structure.[23] However, this previous investigation did not consider the sealing of the UTC. As shown in Fig. 2(a), when a flexible substrate with a UTC is embedded with a sealing material, strain is transmitted to the island structure through both the sealing material and the meander structure. Therefore, we developed a sealing method to realize a floating island structure inside the sealing material. As shown in Fig. 2(b), by forming this floating island structure inside the sealing material, the tensile strain transmitted from the sealing material can be reduced. We named the structure a "floating nested structure".

The objective of this study was to demonstrate the effect of our floating nested structure in reducing the strain propagated to the UTC. This paper first describes the method of fabricating a UTC for tensile testing. Using MEMS technology, we succeeded in fabricating a 5-μm-thick UTC device. The mounting and sealing processes for developing the floating nested structure are next described. Finally, a tensile test was performed on a test sample to demonstrate the reduction in tensile strain propagation by the floating nested structure.

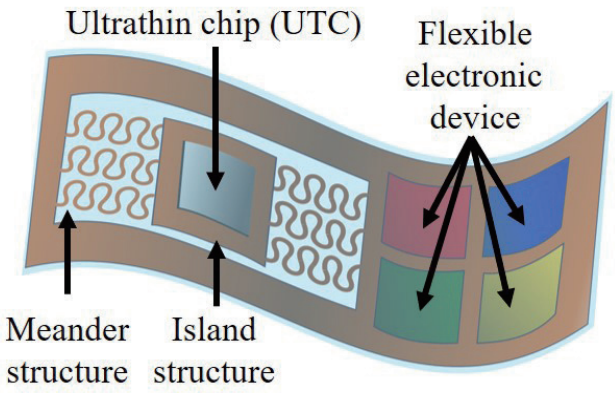

Fig. 1. (Color online) Image of FHE device using UTC.

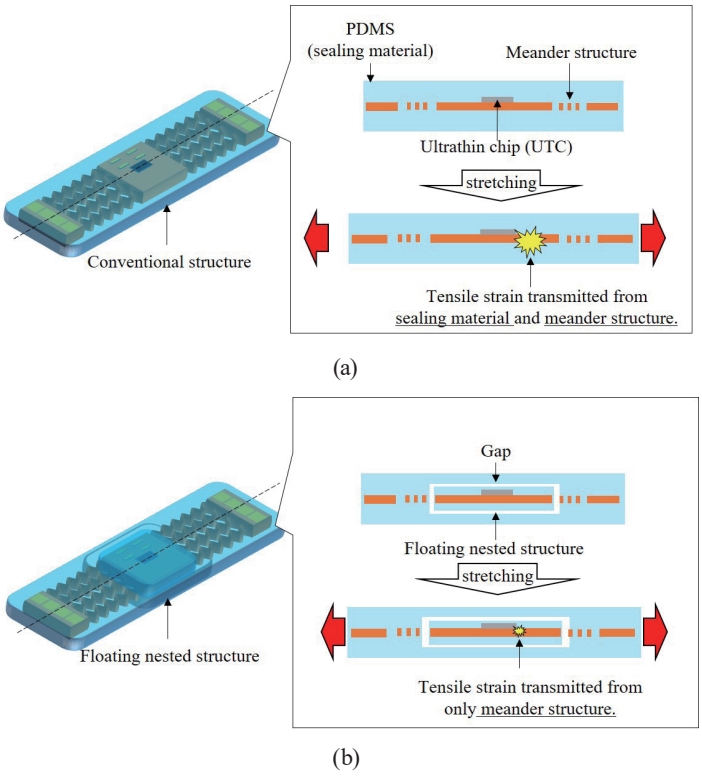

Fig. 2. (Color online) Cross-sectional views of (a) FHE device using conventional sealing structure and (b) FHE device using floating nested structure.

2. Materials and Methods

2.1 Fabrication of UTC

Figure 3(a) shows the process of fabricating the UTC using the MEMS technology and a silicon-on-insulator (SOI) substrate.[24–27] First, platinum and titanium (Pt/Ti) were sputtered on the SOI substrate (step 1). Next, the Pt/Ti layer was milled by ion milling, and a Pt/Ti wire was formed on the device Si layer (step 2). Subsequently, the device Si layer was dry-etched (step 3). After that, the handle Si layer was etched by deep reactive ion etching (deep-RIE). Then, the SiO_2 layer was etched using RIE equipment (step 4). The thicknesses of the Pt/Ti, device Si, SiO_2, and handle Si layers were 200 nm, 5 µm, 1 µm, and 400 µm, respectively. Figure 3(b) shows the structure and a photograph of the fabricated UTC. The size of this UTC was 2×3 mm^2 and its thickness was 5 µm. The chip was supported on the handle Si layer by four support structures. A notch was formed in each support structure, and by breaking this notch, it was possible to pick up only the UTC from the SOI substrate. Figure 4(a) shows the UTC after being released from the SOI substrate. It was confirmed that the UTC could be released from the SOI substrate by breaking the notch. In the UTC, four Pt/Ti wires (wires A, B, C, and D) were formed. The generation of cracks on the UTC can be detected by measuring the resistance of these wires, as discussed later. Additionally, as shown in Fig. 4(b), it was confirmed that the UTC had flexibility and could be bent to a radius of curvature of 0.5 mm.

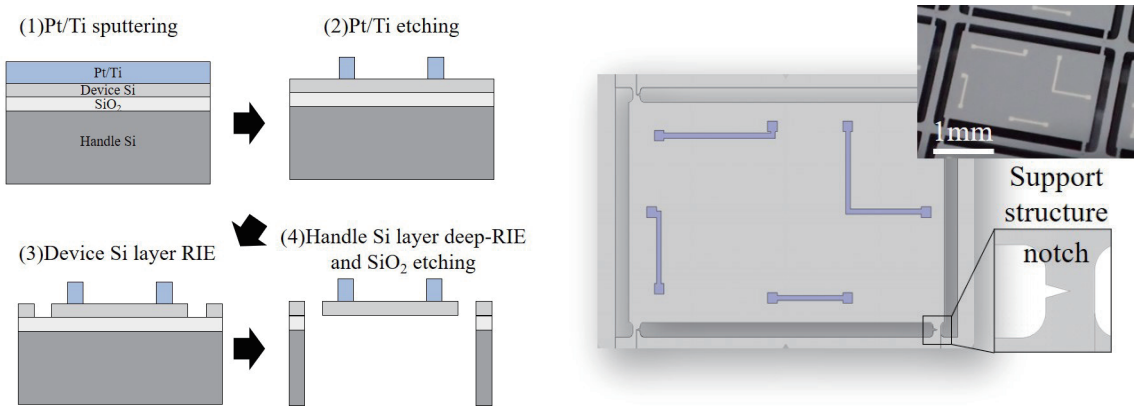

Fig. 3. (Color online) (a) Process of fabricating UTC using MEMS technology and (b) structure of fabricated UTC.

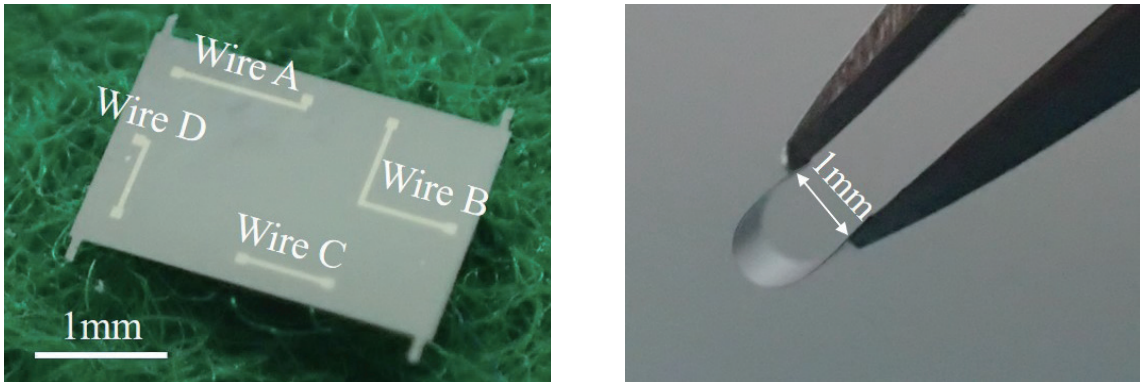

Fig. 4. (Color online) Photographs of (a) UTC after being released from SOI substrate and (b) UTC bent by pin set (radius of curvature: 0.5 mm).

2.2 Floating nested structure

The UTC mounting and sealing processes were carried out as shown in Fig. 5. First, a flexible substrate with an island structure and eight meander structures was fabricated (step 1). The size of this flexible substrate was 45 × 15 mm^2 and its thickness was 125 μm. The flexible substrate material was polyimide (MB18-25-18CEG, Nippon Steel Chemical & Material Co., Ltd., Japan). Copper wires (thickness of 5 μm) were formed on the front side of this flexible substrate by lithography and etching. Subsequently, the flexible substrate was processed using a laser cutter (3500U, EO Technics Co., Ltd., Japan) to form the island structure and meander structures. The size of the island structure was 10 × 10 mm^2. The meander structures were fan-shaped (width: 300 μm, radius of curvature: 1 mm, connection angle: 30°). Next, a UTC was mounted at the center of the surface of the island structure (step 2). Eight bumps were formed

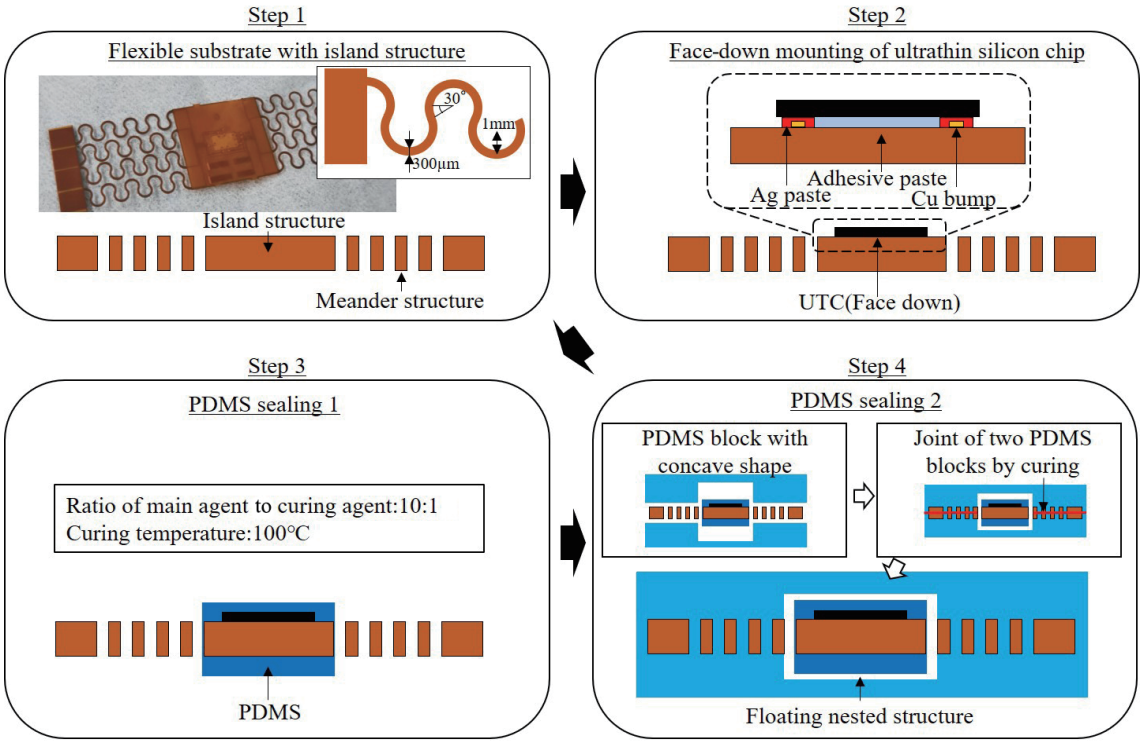

Fig. 5. (Color online) Process of sealing test sample using floating nested structure.

at the center of the island structure and connected to the eight pads at both ends of the flexible substrate through the eight meander structures; first, Ag paste (Rexalpha RA PS 074, Toyo Ink Co., Ltd., Japan) was added dropwise to the bump portion, then adhesive was applied (CA-191, Cemedine Co., Ltd., Japan) to the other portions. After aligning the eight bumps and eight Pt/Ti electrode pads of the UTC, the face-down mounting of the UTC was conducted. Next, the island structure was sealed (step 3); the sealing material was dimethylpolysiloxane (PDMS). The ratio of the main agent to the curing agent, the curing temperature, and the thickness of PDMS were 10:1, 100 °C, and 2 mm, respectively. Finally, the flexible substrate was entirely sealed (step 4) as follows. Two PDMS blocks with a concave shape were created using a mold. The flexible substrate was sandwiched between the two PDMS blocks (thickness of 2.5 mm). Finally, the two PDMS blocks were joined by coating PDMS on the joint surface and curing.

3. Experiment

3.1 Experimental setup

In order to demonstrate that the floating nested structure can reduce tensile strain transmission, an experiment was conducted using test samples with and without a floating

nested structure. Figure 6 shows the experimental setup. To measure the strain during the experiment, a strain gauge (KFGS-2-120-C1-11L5M3R, Kyowa Electronic Instruments Co., Ltd., Japan) was attached to the center of the back side of the island structure using adhesive paste (CC-33A, Kyowa Electronic Instruments Co., Ltd., Japan). Both edges of the test sample were clamped using tensile testing equipment. The strain gauge was connected to the bridge circuit and the measurement system. Enameled wires were soldered to the pads at both edges of the flexible substrate and emerged on the exterior of the test sample. By connecting the enameled wires to the tester, the resistances of wires A, B, C, and D were measured to detect the cracking and breaking of the UTC. The tensile test equipment was connected to a controller and a tensile stress was applied to the test samples by adjusting the distance between the clamps; the initial distance was 60 mm. In this experiment, the elongation was 0–20% (clamp distance from 60 to 72 mm). The strains and resistances of wires A, B, C, and D were measured at every 2.5% elongation.

3.2 Results

Figure 7(a) presents the results obtained by the tensile test for test sample A, and Fig. 7(b) presents the results obtained by the stretching test for test sample B. For test sample A, as the elongation increased, the value indicated by the strain gauge also increased. When the elongation was 20%, the strain was 710 με. For test sample B, the strain increased with the

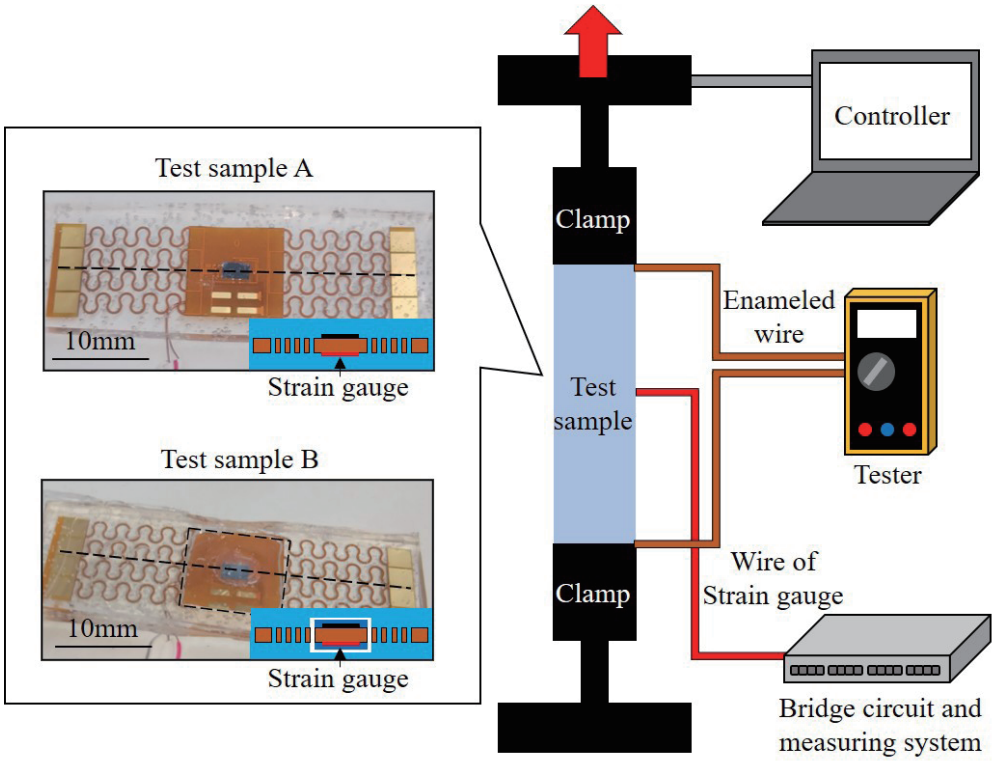

Fig. 6. (Color online) Experimental setup.

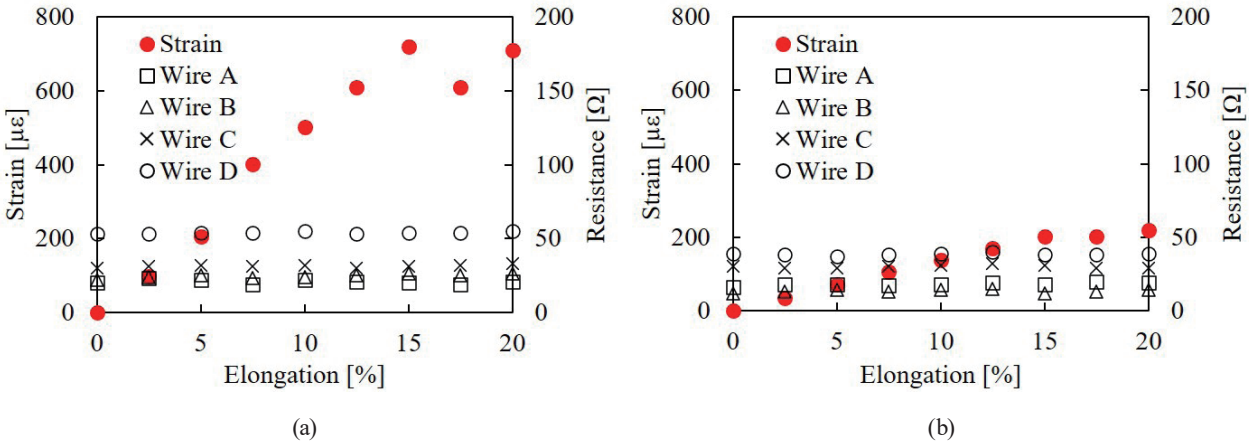

Fig. 7. (Color online) Experimental results of (a) test sample A and (b) test sample B.

elongation rate. However, the rate of increase was smaller than that for test sample A. When the elongation was 20%, the strain of test sample B was only 220 με because the floating nested structure reduced the tensile strain transmitted through the PDMS sealing. When the elongation was 20%, the reduction was 69.0%. Regarding the resistances of wires A, B, C, and D of the UTC, there was no significant change in the resistance of each wire, even when the elongation was 20%. Therefore, it was concluded that the UTC did not crack or break. Note that when the elongation reached 22.5%, a crack was generated on the PDMS block of test sample A. Then, this experiment was stopped. A detailed discussion of these results is presented in the next section.

4. Discussion

This paper presents a newly developed sealing technology for an FHE device with flexibility and stretchability. We also propose a sealing method using a floating nested structure. From the experimental results, the floating nested structure can reduce the transmission of tensile strain. The tensile strains when the conventional sealing structure and floating nested structure were 710 and 220 με, respectively; then the elongation was 20%. This means that the floating nested structure can reduce strain transmission by 69.0%.

First, regarding the experimental results of test sample A, the strain increased proportionally to the elongation up to 15%, but then suddenly dropped when the elongation reached 17.5%. This may have been caused by the partial peeling of the interface between the PDMS and the flexible substrate. A shearing force was applied to the interface between the PDMS and the flexible substrate owing to the elongation of the test sample. When the shearing force reached its limit, a lateral slip occurred, which reduced the transmission of the tensile strain. However, because the peeling was partial, the elongation increased to 20%.

Regarding the experimental results of test sample B, although the rate of increase in tensile strain was smaller than that of test sample A, the tensile strain increased proportionally to

the elongation. There were two causes of tensile strain propagation, namely, the meander structure and the friction of the PDMS blocks. With regard to the meander structure, the limit to which propagation can be reduced depends on the shape of the structure. Therefore, tensile strain propagation can be further reduced by optimizing the shape of the meander structure. With regard to the friction of the PDMS blocks, it is considered that strain propagation can be suppressed by enclosing a lubricating liquid inside the floating nested structure.

Finally, with regard to the experimentally observed UTC stress, the stresses applied to the UTC were 121.0 MPa (test sample A) and 37.2 MPa (test sample B), and Young's modulus for silicon was assumed to be 169 GPa;[27] the strain was the same on the front and back sides of the flexible substrate. Considering that the tensile breaking stress of single-crystal silicon was 1.89 GPa, the stress applied to the UTC did not reach the breaking stress in this experiment. Therefore, the wires in the UTC did not break.

The following conclusions were drawn from the above results.

(1) When the elongation was 20%, the tensile strain of test sample A (sealing structure without a floating nested structure) was 710 με and that of test sample B (with a floating nested structure) was 220 με.
(2) A strain reduction of 69.0% was achieved owing to the floating nested structure.
(3) By optimizing the meander structure and reducing the friction of the sealing materials, the strain propagation may be further reduced.
(4) The UTC did not break at 20% elongation because the stress did not reach the breaking stress of silicon. However, this may occur with a larger elongation.

5. Conclusions

We proposed a novel sealing structure for developing flexible and stretchable FHE devices using a UTC. The proposed sealing structure can reduce the tensile strain propagating from the sealing structure. Although this study focused on a UTC, it is considered that this structure can also be used to reduce the tensile strain of the sealing of packaged chips. Therefore, the floating nested structure has good potential for application to the development of FHE devices. In future works, a vital-sign sensor will be fabricated on the floating nested structure and a test will be conducted to demonstrate the effectiveness of the structure.

Acknowledgments

We would like to give heartfelt thanks to Mr. Tsuda (Yamagata University) who helped us with the experiment in this study. This work was conducted as one of the research topics of the New Energy and Industrial Technology Development Organization (NEDO) project.

References

1 T. Takeshita, M. Yoshida, Y. Takei, A. Ouchi, A. Hinoki, H. Uchida, and T. Kobayashi: Sci. Rep. **9** (2019) 1. https://doi.org/10.1038/s41598-019-42027-x
2 Y. Yamamoto, D. Yamamoto, M. Takada, H. Naito, T. Arie, S. Akita, and K. Takei: Adv. Healthcare Mater. **6** (2017) 1. https://doi.org/10.1002/adhm.201700495

3 A. C. Myers, H. Huang, and Y. Zhu: RSC Adv. **5** (2015) 11627. https://doi.org/10.1039/C4RA15101A
4 J. Kim, P. Gutruf, A. M. Chiarelli, S. Y. Heo, K. Cho, Z. Xie, A. Banks, S. Han, K. I. Jang, J. W. Lee, K. T. Lee, X. Feng, Y. Huang, M. Fabiani, G. Gratton, U. Paik, and J. A. Rogers: Adv. Funct. Mater. **27** (2017) 1. https://doi.org/10.1002/adfm.201604373
5 J. Kim, N. Kim, M. Kwon, and J. Lee: ACS Appl. Mater. Interfaces **9** (2017) 25700. https://doi.org/10.1021/acsami.7b05264
6 J. W. Jeong, W. H. Yeo, A. Akhtar, J. J. S. Norton, Y. J. Kwack, S. Li, S. Y. Jung, Y. Su, W. Lee, J. Xia, H. Cheng, Y. Huang, W. S. Choi, T. Bretl, and J. A. Rogers: Adv. Mater. **25** (2013) 6839. https://doi.org/10.1002/adma.201301921
7 K. I. Jang, K. Li, H. U. Chung, S. Xu, H. N. Jung, Y. Yang, J. W. Kwak, H. H. Jung, J. Song, C. Yang, A. Wang, Z. Liu, J. Y. Lee, B. H. Kim, J. H. Kim, J. Lee, Y. Yu, B. J. Kim, H. Jang, K. J. Yu, J. Kim, J. W. Lee, J. W. Jeong, Y. M. Song, Y. Huang, Y. Zhang, and J. A. Rogers: Nat. Commun. **8** (2017) 1. https://doi.org/10.1038/ncomms15894
8 Y. Takei, T. Takeshita, M. Yoshida, and T. Kobayashi Jpn. J. Appl. Phys. **58** (2019) 1. https://doi.org/10.7567/1347-4065/ab3e52
9 W. Iwasaki, H. Nogami, S. Takeuchi, M. Furue, E. Higurashi, and R. Sawada: Sensors **15** (2015) 25507. https://doi.org/10.3390/s151025507
10 H. Nogami, W. Iwasaki, T. Abe, Y. Kimura, A. Onoe, E. Higurashi, S. Takeuchi, M. Kido, M. Furue, and R Sawada: Proc. IMechE **225** (2010) 411. https://doi.org/10.1243/09544119JEIM727
11 A. Koh, S. R. Gutbrod, J. D. Meyers, C. Lu, R. C. Webb, G. Shin, Y. Li, S. K. Kang, Y. Huang, I. R. Efimov, and J. A. Rogers: Adv. Healthcare Mater. **5** (2016) 373. https://doi.org/10.1002/adhm.201500451
12 T. Yokota, Y. Inoue, Y. Terakawa, J. Reeder, M. Kaltenbrunner, T. Ware, K. Yang, K. Mabuchi, T. Murakawa, M. Sekino, W. Voit, T. Sekitani, and T. Someya: PNAS **112** (2015) 14533. https://doi.org/10.1073/pnas.1515650112
13 W. Wu: Nanoscale **9** (2017) 7342. https://doi.org/10.1039/C7NR01604B
14 A. M. Hussain and M. M. Hussain: Adv. Mater. **28** (2016) 4219. https://doi.org/10.1002/adma.201504236
15 S. Gupta,W. T. Navaraj, L. Lorenzelli, and R. Dahiya: NPJ Flexible Electron. **2** (2018). https://doi.org/10.1038/s41528-018-0021-5
16 M. M. Hussain, J. P. Rojas, and G. A. T. Sevilla: Proc. SPIE Defense, Security, and Sensing (SPIE, 2013) 87251M. https://doi.org/10.1117/12.2015551
17 D. Shahrjerdi and S. W. Bedell: Nano. Lett. **13** (2013) 315. https://doi.org/10.1021/nl304310x
18 G. A. T. Sevilla, M. T. Ghoneim, H. Fahad, J. P. Rojas, A. M. Hussain, and M. M. Hussain: ACS Nano **8** (2014) 9850. https://doi.org/10.1021/nn5041608
19 J. D. Brand, M. D. Kok, M. Koetse, M. Cauwe, R. Verplancke, F. Bossuyt, M. Jablonski, and J. Vanfleteren: Solid State Electron. **113** (2015) 116. https://doi.org/10.1016/j.sse.2015.05.024
20 T. Sterken, J. Vanfleteren, T. Torfs, M. O. D. Beeck, F. Bossuyt and C. V. Hoof: Proc. Annu. Int. Conf. IEEE Engineering in Medicine and Biology Society (IEEE, 2011) 6886. https://doi.org/10.1109/IEMBS.2011.6091734.
21 R. Xu, J. W. Lee, T. Pan, S. Ma, J. Wang, J. H. Han, Y. Ma, J. A. Rogers, and Y. Huang: Adv. Funct. Mater. **27** (2017) 1604545. https://doi.org/10.1002/adfm.201604545
22 M. Jablonski, R. Lucchini, F. Bossuyt, T. Vervust, J. Vanfleteren, J.W.C. De Vries, P. Vena, and M. Gonzalez: Microelectron. Reliab. **55** (2015) 143. https://doi.org/10.1016/j.microrel.2014.09.009
23 T. Takeshita, Y. Takei, T. Yamashita, A. Oouchi, and T. Kobayashi: Flexible Printed Electron. **5** (2020) 1. https://doi.org/10.1088/2058-8585/ab7bc3
24 T. Yamashita, H. Okada, T. Itoh, and T. Kobayashi: Jpn. J. Appl. Phys. **54** (2015) 1. https://doi.org/10.7567/JJAP.54.10ND08
25 T. Yamashita, H. Okada, T. Itoh, and T. Kobayashi: IEEE Sens. J. **16** (2016) 8840. https://doi.org/10.1109/JSEN.2016.2578936
26 T. Takeshita, T. Yamashita, N. Makimoto, and T. Kobayashi: Jpn. J. Appl. Phys. **56** (2017) 1. https://doi.org/10.7567/JJAP.56.10PF11
27 S. Lee, J. H. Kim, T. Ohba, Y. S. Kim, and T. S. Kim: Proc. ICEP-IAAC (JIEP, 2018) 339. https://doi.org/10.23919/ICEP.2018.8374318